processes

MDPI

Article

Experimental Investigation on Ignition of Hyperburner Based on Gliding Arc Plasma Igniter Driven by Pressure Difference

Xinyao Cheng, Huimin Song *, Jiulun Sun, Wei Cui, Zhibo Zhang, Min Jia, Di Jin and Yifei Zhu

Science and Technology on Plasma Dynamics Laboratory, Air Force Engineering University, Xi'an 710038, China
* Correspondence: min_cargi@sina.com

Abstract: The hyperburner is a key component of a TBCC engine, and its reliable ignition and stable operation are critical. The gliding arc plasma igniter driven by differential pressure has the technical advantages of low energy consumption and high jet temperature. In this paper, the electrical and flow characteristics of the gliding arc plasma igniter are studied, and the basic ignition experiment in the hyperburner is carried out. Electrical characteristic experiments show that the discharge duration, the evolution of the gliding arc and the fracture frequency are affected by the pressure difference between the inlet and outlet of the igniter (Δp). With the increase in Δp, the frequency of the trapezoidal envelope in the voltage and current waveforms increases, and the frequency of the evolution and fracture of the gliding arc increases. The continuous discharge time of the gliding arc decreases when Δp = 550 Torr. The flow characteristic experiments show that the velocity of the swirl sheath is increased and the protective effect on the gliding arc is enhanced with the increase in Δp. In the range of 20–550 Torr, the jet length first increases and then decreases with the increase in Δp. The jet length reaches a maximum of 31 mm at Δp = 50 Torr. Basic ignition experiments show that proper Δp can widen the lean ignition limit and shorten the ignition delay time. In the working conditions of this paper, the ignition effect is the best when Δp = 350 Torr, which can widen the lean ignition limit by 37.5% and shorten the ignition delay time by 17%. After increasing the oil–gas ratios, the combustion is more complete and the ignition delay time can be shortened by 93.1% at most.

Keywords: gliding arc plasma; hyperburner; jet length; lean ignition limit; ignition process

Citation: Cheng, X.; Song, H.; Sun, J.; Cui, W.; Zhang, Z.; Jia, M.; Jin, D.; Zhu, Y. Experimental Investigation on Ignition of Hyperburner Based on Gliding Arc Plasma Igniter Driven by Pressure Difference. *Processes* **2022**, *10*, 1886. https://doi.org/10.3390/pr10091886

Academic Editors: Richard Lenhard, Jozef Jandačka and Ladislav Dzurenda

Received: 27 July 2022
Accepted: 2 September 2022
Published: 17 September 2022

1. Introduction

With the continuous development of modern warfare, military aircraft need to gain altitude and speed advantages in combat, expand the flight envelope, obtain favorable fighter aircraft characteristics, and avoid sources of danger. However, a single type of engine can no longer meet all flight needs. Based on existing technology, a turbine-based combined cycle (TBCC) engine formed by the combination of a turbojet and a ramjet is considered to be the most promising power solution [1,2].

In recent years, because TBCC engines have advantages such as a wider flight envelope than turbojets, higher specific impulse than rocket engines, and reusability, there have been rapid developments in this area of research [3–5]. According to the combination of turbojet and ramjet, there are two types of TBCC engines: tandem and parallel [6]. The tandem TBCC engine is the more widely studied combined power scheme owing to advantages such as its compact structure, light weight, and low wind resistance. The J58 engine used by the American "Blackbird" reconnaissance aircraft is considered to be the earliest tandem TBCC engine in the world [7–9]. The highest flight Mach number of the "Blackbird" reconnaissance aircraft exceeds 3 Ma, and the flight altitude can reach 30 km, which highlights the excellent performance of the tandem TBCC engine and provides valuable experience for future TBCC engine research [10].

The stable operation of the tandem TBCC engine depends on a key component, namely the hyperburner. The hyperburner of the tandem TBCC engine is a combustion chamber

formed by the combination of an afterburner and a ramjet. For example, the hyperburner of the Japanese RTA-1 engine is in the turbofan mode when the Mach number is less than 3 Ma, and the hyperburner acts as an afterburner to provide thrust; when the Mach number exceeds 3 Ma, it enters the ram mode, and the hyperburner acts as a ramjet to provide thrust [11]. Compared with the traditional engine, the ignition conditions of the hyperburner are more severe, which makes the ignition and flame transfer more difficult in the hyperburner. In order to achieve stable ignition, widen the lean ignition limit, and shorten the ignition delay time of the hyperburner, it is crucial to investigate a new ignition method for the hyperburner.

In recent years, plasma technology has been developing rapidly and showing its unique advantages. In material handling, Dimitrakellis et al. [12] found a fast hydrophilization with gliding arc plasma discharges when measuring water contact angle measurements on gliding arc plasma treated epoxy samples. In the production of gas, Yin Pang et al. [13] experimentally investigated the influence of nonthermal plasma (NTP) application on the reaction kinetics of atmospheric pressure steam gasification of charcoal using a thermostatically controlled drop tube reactor. The experiment revealed that the plasma enhanced the reaction rate coefficients by 27%. In addition, plasma ignition technology has also been studied in depth. The study by Brande et al. [14] is the earliest reported research on the application of an electric field to a flame. Equilibrium plasma affects the reaction rate by increasing the gas temperature, and the common form of application is spark plug ignition [15–18]; non-equilibrium plasma has a higher electron temperature, which can change the reaction pathway of combustible matter to increase the chemical reaction rate [19–21]. Gliding arc plasma has the characteristics of both equilibrium and non-equilibrium plasma, and it realizes the effect of ignition and combustion through three major effects [22–25]. As the gliding arc generator has a low energy consumption and high jet temperature, in recent years, an increasing number of researchers have performed experimental research on the application of gliding arc plasma in ignition and combustion. Ombrello et al. [26,27] studied the ignition enhancement effect of magnetically gliding arc discharge on methane–air hedge flames, found that the gliding arc can increase the flame elongation rate, and reported that the enhanced ignition of the gliding arc at low temperatures mainly comes from the thermal effect. Leonov et al. [28–30] conducted research on quasi-DC discharge arcs in a supersonic flow and reported that plasma can enhance mixing and change the flow field. Pinto et al. [31] conducted ignition experiments on natural gas–air mixtures using a DC gliding arc and found that the discharge repetition frequency of the gliding arc increased with an increase in fuel concentration. Jia et al. [32] investigated gliding arc plasma ignition in a double-head swirling combustor. The experiments showed that single-channel gliding arc plasma can broaden the lean ignition limit by approximately 67% compared with the traditional spark igniter. Chen et al. [33] investigated the characteristics of gliding arc plasma at different flow rates and its control effect on the static instability of the swirl flame. The experiment showed that the lean blowout limits increased when the flame mode changed from stable to pulsating, and decreased significantly after the application of the gliding arc plasma.

Gliding arc plasma is widely used in turbine engine combustion and ramjet combustion chambers and has achieved excellent results. However, research on the application of plasma to the hyperburner is still in the exploratory stage, and there is no published literature on the realization of hyperburner ignition and stable combustion by gliding arc plasma. In order to make the gliding arc igniter perform fully in the hyperburner, it is necessary to explore the electrical characteristics, jet characteristics, and outlet flow field characteristics of the gliding arc igniter before carrying out the ignition experiments. Therefore, the electrical characteristics, outlet flow field, and jet characteristics of the gliding arc plasma igniter were investigated in this study. Finally, experimental research on gliding arc plasma ignition in the hyperburner was carried out in this study.

2. Experimental System

The experimental system is composed of a gliding arc plasma ignition system driven by a pressure difference, a characteristic experimental system, and a hyperburner ignition experimental system.

2.1. Gliding Arc Plasma Generation System Driven by Pressure Difference

The gliding arc plasma generation system consists of a gliding arc plasma igniter driven by pressure air, a power supply, and air cylinders.

The schematic diagram of the gliding arc plasma igniter driven by pressure difference is shown in Figure 1, and it is mainly composed of the cylindrical anode, the cathode inner core, the igniter shell, the ceramics, and the air supply sleeve. When the igniter is working, the pressure at the inlet of the gas supply sleeve is greater than the outlet pressure of the cathode channel, and a pressure difference is formed between the inlet and outlet of the igniter. The airflow enters the igniter from the air supply sleeve. After the combined action of the swirl hole and the convergent section, a swirling airflow blows out from the cathode channel with both axial and circumferential speed. When the igniter is energized, the electric field strength between the anode and cathode exceeds the breakdown field strength of air. The air will be broken down at the shortest distance between the anode head and the cathode inner core convergent section to form an arc. Because of aerodynamic forces, the arc will be continuously rotated and stretched along the inner wall of the cathode channel to form a gliding arc and will be blown out of the cathode channel.

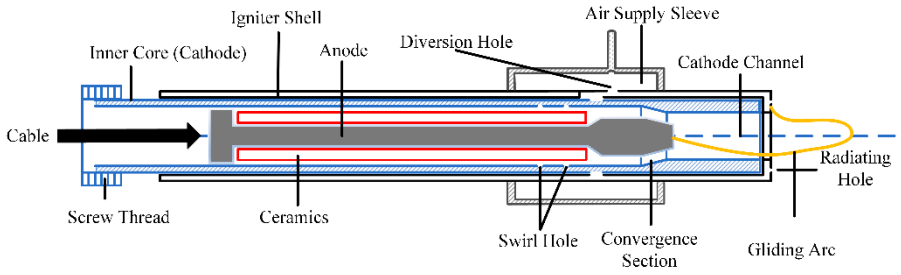

Figure 1. Gliding arc plasma igniter driven by pressure difference.

The power supply is a laboratory-made gliding arc plasma igniter power supply. The output waveform of the power supply is approximately a modulated sine wave, with a single-cycle duration of 100 ms, of which the waveform time span was 10 ms and the duty cycle was 10%.

Air cylinders with an oxygen concentration of 21% were used as the air supply system.

2.2. Characteristic Experimental System

The characteristic experimental system of the gliding arc plasma igniter driven by a pressure difference is composed of the particle image velocimetry (PIV) system and the data acquisition system, as shown in Figure 2.

The TABOR-D30 Zhuo Lei laser with a pulse energy of 30 mJ and a wavelength of 527 nm was used in the PIV system. The Phantom-v2512 camera was used as the high-speed camera, with a field of view of 1280 × 800 pixels and a maximum acquisition frequency of 200 Hz.

Data acquisition systems included a high-speed camera, pressure sensors, an oscilloscope, a voltage probe, and a current probe. The Phantom-V2512 camera was also used in the jet characteristic experiment, where the resolution was set to 384 × 288, the exposure time was set to 34 μs, and the shooting speed was set to 25,000 fps. The TA3351GP5S22M3B3 was used as a pressure sensor, and it had a range of 0-200 KPa and an accuracy of 0.075%. The Tektronix P6015A and the Tektronix P6021 were respectively used as voltage probes and current probes to acquire voltage and current signals. The Tektronix DPO4104 was used as an oscilloscope to display the voltage and current waveforms in real time.

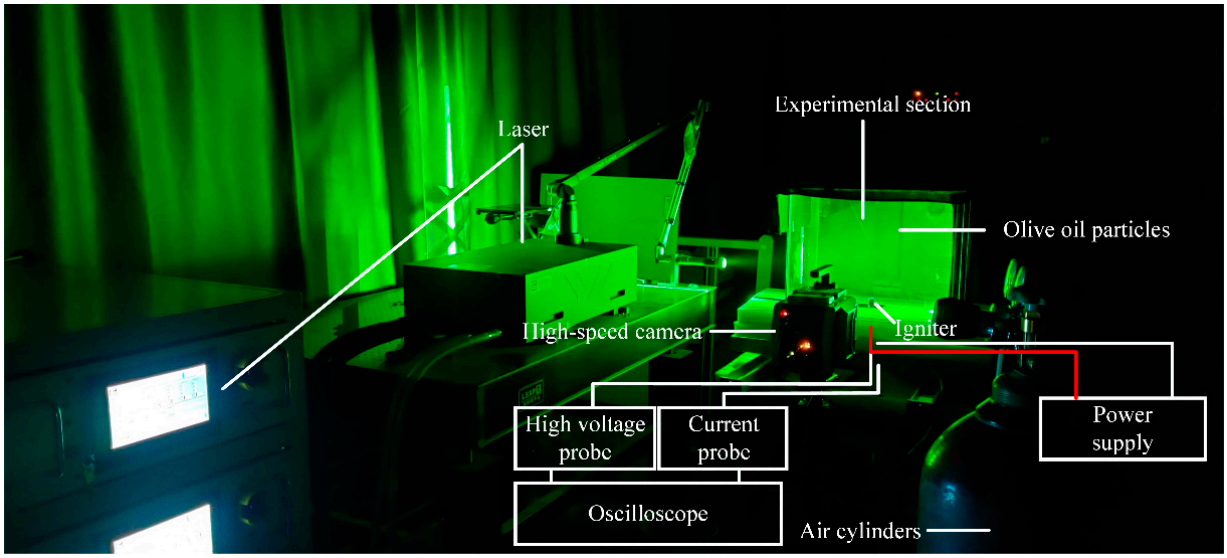

Figure 2. Characteristic experimental system.

2.3. Hyperburner Ignition Experimental System

The hyperburner ignition experimental system is composed of a hyperburner test bench, a medium supply system, and a data acquisition system. The schematic diagram of the structure is shown in Figure 3a, and the actual picture is shown in Figure 3b.

The hyperburner test bench includes an inlet section, an experimental section, and an exhaust section. In the inlet section, an electric heater with a maximum output of 200 kW is used to adjust the incoming flow temperature. The cross-sectional area of the experimental section is 180 mm (height) × 150 mm (width). A hyperburner-integrated flame stabilizer was placed in the experimental section, and the schematic diagram is shown in Figure 4. A throat was placed in the exhaust section to adjust the maximum Mach number.

The working principles of the hyperburner-integrated flameholder are as follows: When the mainstream hot gas blows to the hyperburner-integrated flameholder, part of the hot gas enters the intake pipe of the vaporizer and blows out from the injector hole carrying kerosene droplets. Kerosene is sprayed from a 0.5 mm diameter round hole at the tip of the oil supply pipe, achieving pressure atomization. The sprayed kerosene touches the intake pipe of the vaporizer, and the kerosene droplets are shattered. Finally, as the kerosene droplets are carried by the hot gas, they are atomized by absorbing the heat of the hot gas, and they are also broken up again by the shear force when they are taken along by hot gas. Eventually, liquefaction and evaporation of the kerosene droplets are realized.

The medium supply system provides the air medium and the kerosene medium for the experiment to ensure the smooth progress of the experiment.

The data acquisition system collects the total temperature of the incoming flow, the total pressure of the experimental section, the static pressure of the experimental section, the static pressure of the igniter inlet, and the flow of kerosene in real time. The Photron UX50 was used as a high-speed camera in the ignition experiment; the resolution was set to 1280 × 296, and the shooting speed was set to 5120 fps.

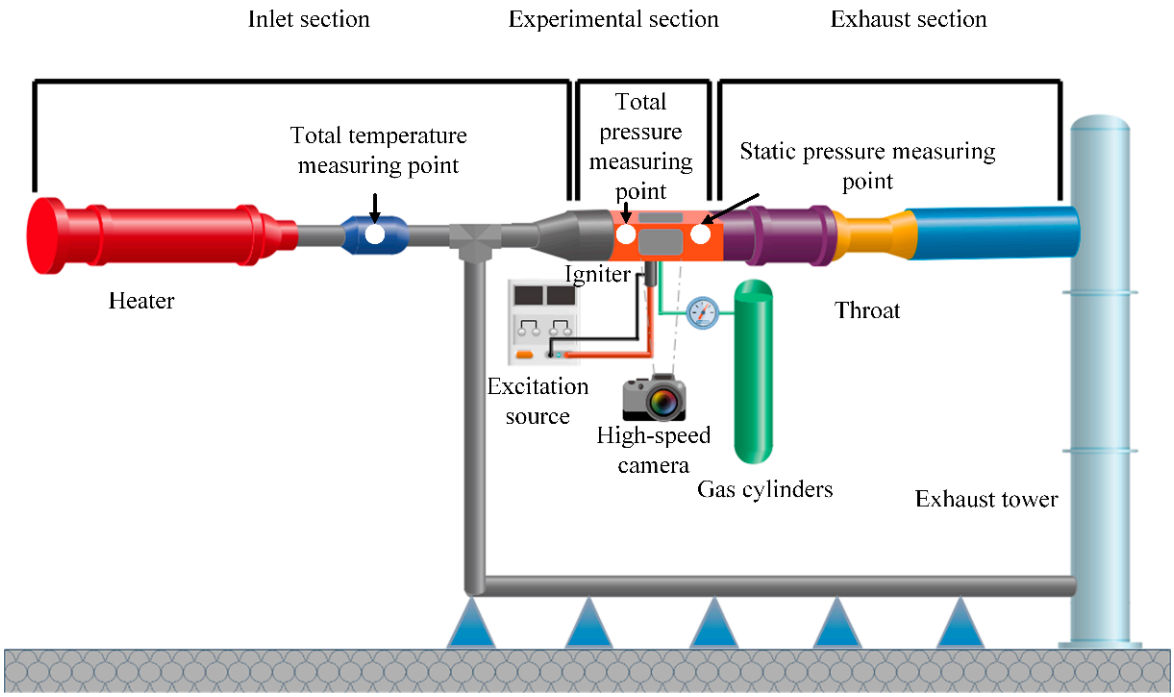

(**a**)

(**b**)

Figure 3. Hyperburner ignition experimental system: (**a**) schematic; (**b**) physical map.

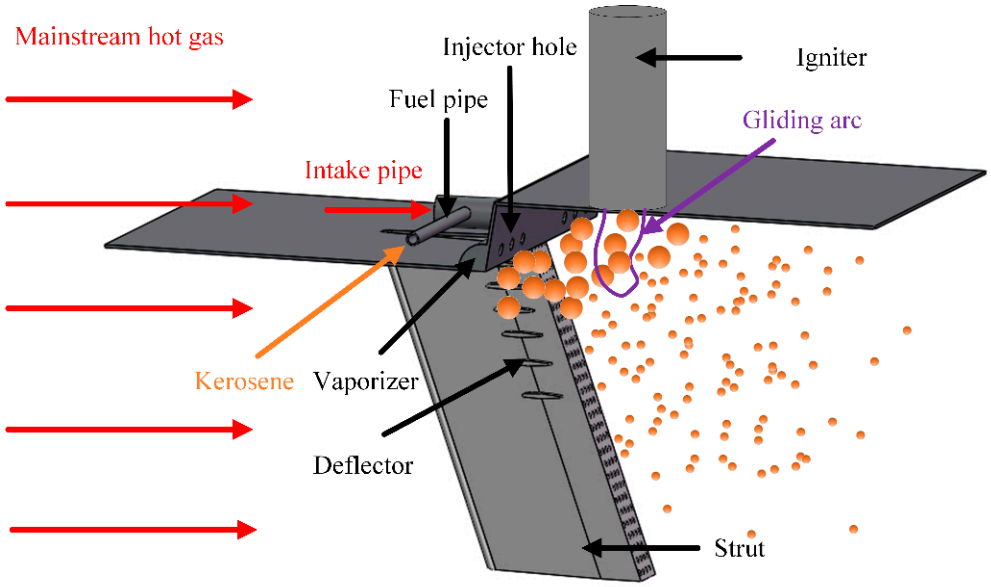

Figure 4. Hyperburner-integrated flameholder structure.

3. Experimental Results and Analysis

3.1. Electrical Characteristics of the Gliding Arc Plasma Igniter

When the pressure difference between the inlet and outlet of the igniter (Δp) is 350 Torr, the discharge waveform of the gliding arc plasma igniter is as shown in Figure 5. The single-cycle working time of the gliding arc plasma power supply is 10 ms, which can be divided into a high-voltage breakdown mode (Mode A) and a low-voltage sustaining mode (Mode B). After the power supply begins to work, it first enters Mode A, and the potential difference between the cathode and anode of the igniter increases. When the potential difference exceeds the minimum voltage required for the air gap to be broken down, the arc is generated at the smallest gap between the cathode and the anode. Under the action of the airflow, it is continuously rotated and stretched to form a gliding arc discharge. At this time, the power supply shifts to Mode B, and the excitation voltage exhibits an obvious trapezoidal envelope in Mode B. This is because the Mode B operation included the gliding arc evolution stage and the gliding arc fracture stage. The voltage waveform of 2–3 ms is shown in Figure 6. In the evolution stage of the gliding arc, the excitation voltage increases with the lengthening of the gliding arc. When the voltage reaches the peak value of the trapezoidal envelope, the instantaneous power generated by the power supply is soon unable to meet the instantaneous power required for the maintenance of the gliding arc. At the fracture boundary, the gliding arc continues to elongate owing to the aerodynamic force, and the gliding arc is broken. After the gliding arc is broken, a short-cutting event occurs in the middle of the arc. At this time, a new gliding arc is formed and the evolution process is repeated, as shown in Figure 7. After Mode B ends, the output voltage of the power supply decreases to 0 V, and the gliding arc is extinguished during the rest period of 90 ms.

Figure 8 shows the voltage and current waveforms of the gliding arc plasma igniter at a Δp value of 20 Torr and a Δp value of 550 Torr. A comparison of the voltage and current waveforms for Δp values of 20 Torr, 350 Torr, and 550 Torr shows that the frequency of gliding arc evolution and fracture increases when Δp and the number of trapezoidal envelopes increase. When Δp is 20 Torr, the frequency of gliding arc evolution and fracture in one cycle is 400 Hz, and when Δp is 550 Torr, the frequency of gliding arc evolution and fracture is 2800 Hz (600% faster than when Δp is 20 Torr). In addition, the experimental results show that Δp will affect the duration of the gliding arc discharge. When Δp is 550 Torr, the voltage waveform is normal but the current waveform is 0 A in stage C, which means that the gliding arc is extinguished at this period. The main reason for this

phenomenon is that when Δp is relatively large, the gliding arc is continuously elongated under the action of the airflow, and when the instantaneous power output of the power supply cannot maintain the gliding arc, the discharge is extinguished. However, in Mode B, the voltage peak value is relatively low and cannot reach the minimum voltage required to break down the air gap, so the gliding arc cannot be regenerated. Under the condition of Δp of 550 Torr, the duration of the C stage can reach 1.6 ms, which may weaken the ignition effect of the gliding arc. In practical applications, the flow capacity design of the ducts inside and outside the hyperburner can be carried out according to the effect pattern of Δp on the duration of the gliding arc discharge in order to achieve a better ignition effect.

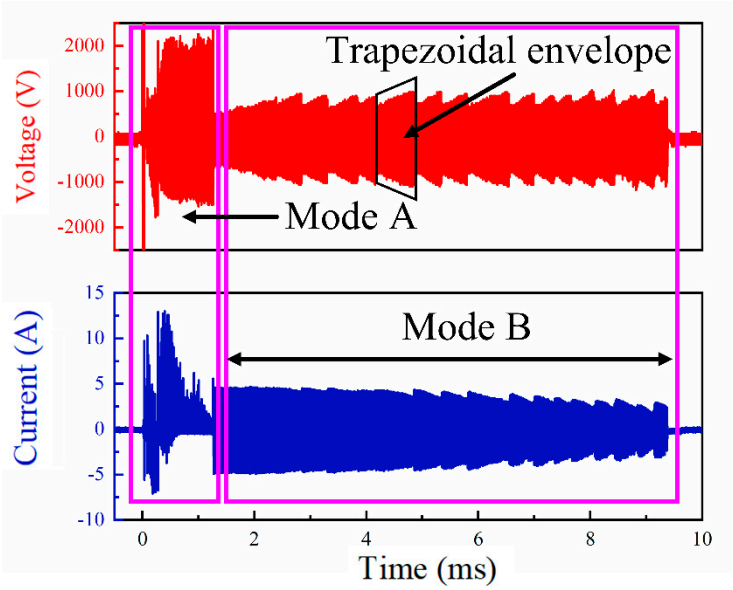

Figure 5. Voltage and current waveforms of gliding arc plasma igniter at Δp = 350 Torr.

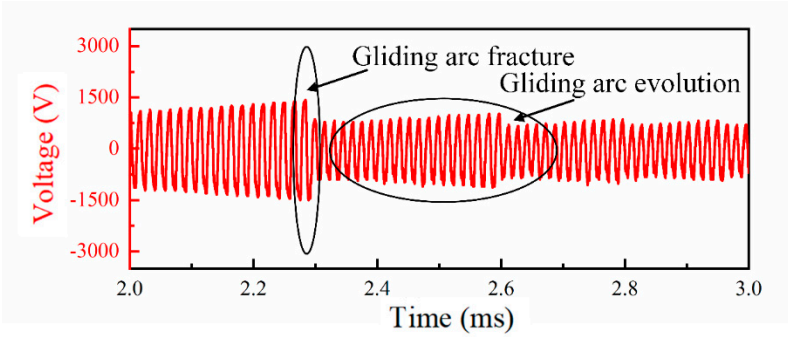

Figure 6. The voltage waveform of 2–3 ms.

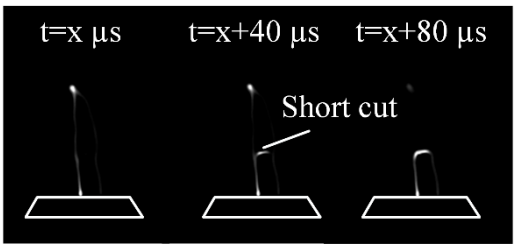

Figure 7. Short-cutting of the gliding arc.

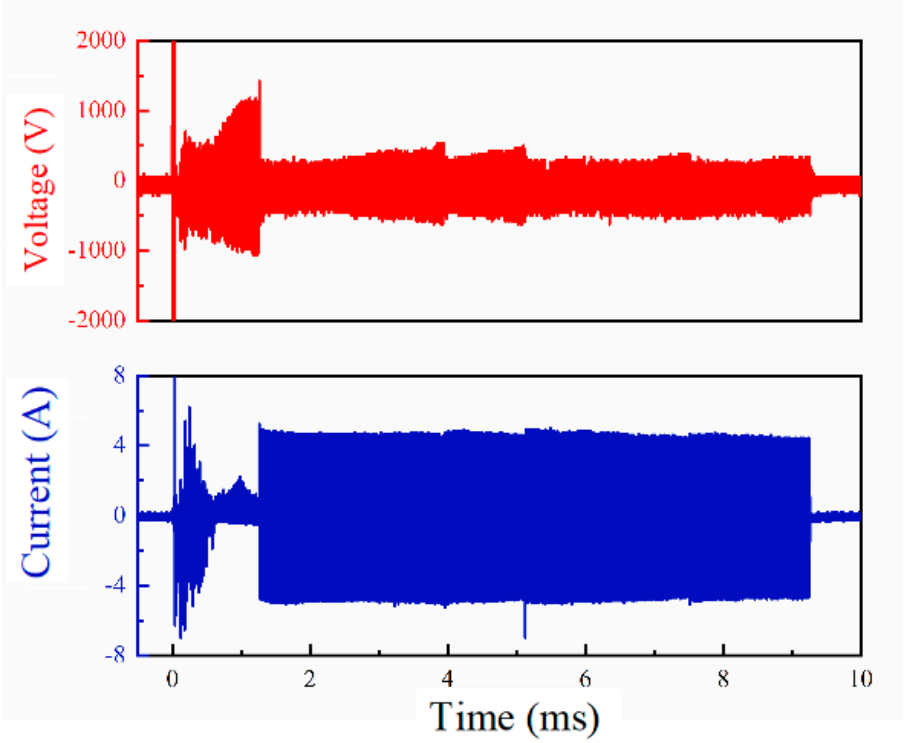

(**a**)

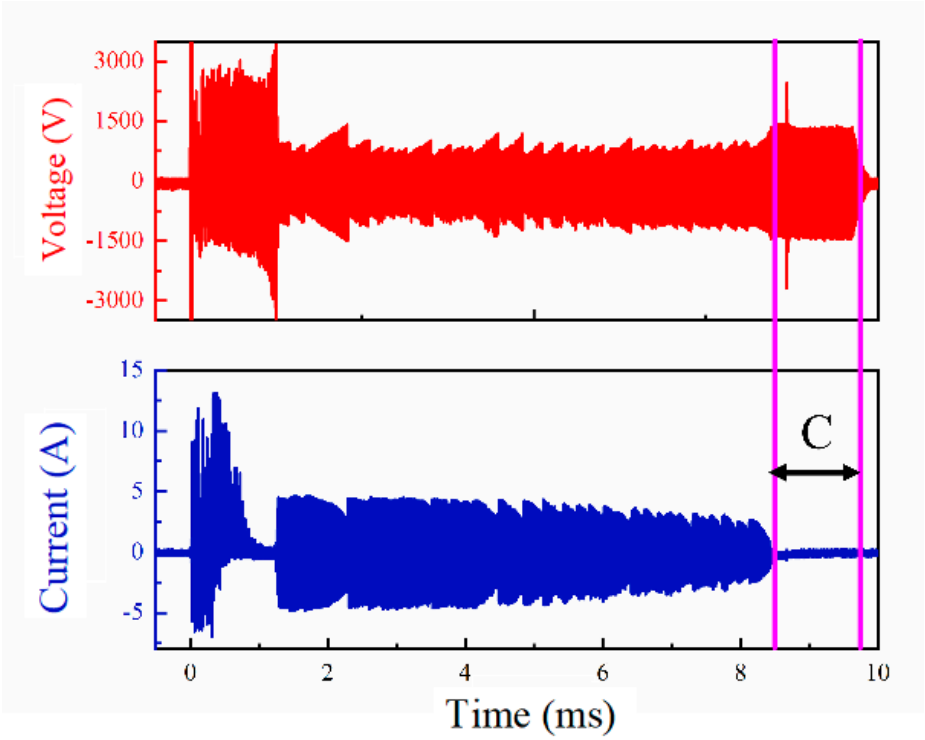

(**b**)

Figure 8. Voltage and current waveforms at Δp = 20 Torr and Δp = 550 Torr: (**a**) voltage and current waveforms at Δp = 20 Torr; (**b**) voltage and current waveforms at Δp = 550 Torr.

3.2. Outlet Flow Field Distribution of Gliding Arc Plasma Igniter

When Δp is 350 Torr, the PIV experimental results of the flow field at the igniter outlet are as shown in Figure 9. Experiments show that when Δp is 350 Torr, the gas ejects from the cathode channel of the igniter and diffuses outward. The velocity gradually

decreases along the axial direction, and the maximum velocity at the outlet is approximately 35 m/s. Because the pressure at the outlet of the igniter is high and the external pressure is low, the gas will diffuse from the place of high pressure to the place of low pressure. Therefore, the gas ejected from the cathode channel will diffuse outward, and as the axial distance increases, the axial velocity decreases. The figure shows that the velocity inside the trapezoidal area is very small, which is caused by the gas ejected from the igniter channel affecting the distribution of the tracer particles and is not the actual velocity in this area.

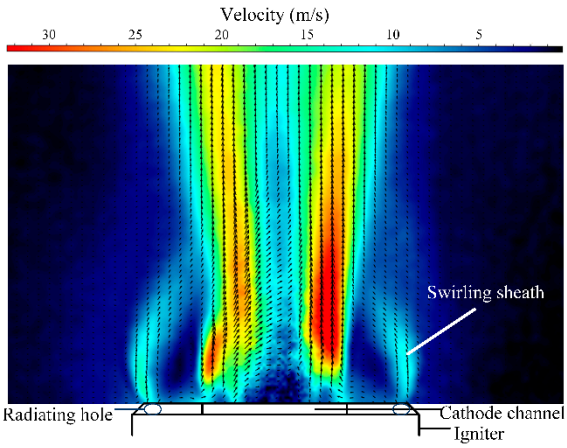

Figure 9. Igniter outlet flow field at Δp = 350 Torr.

Because of the radiating holes on the igniter shell, the outside air will form a swirl sheath through the radiating holes. The swirl sheath will protect the airflow field at the igniter outlet. When Δp is 350 Torr, the gas ejected from the radiating holes will form an elliptical swirl sheath with a maximum speed of about 12 m/s to protect the gliding arc.

Figure 10 shows the maximum airflow velocity at the outlet of the cathode channel of the igniter and the maximum velocity of the swirl sheath under different Δp conditions. With the increase in Δp, the maximum airflow velocity at the outlet of the igniter cathode channel and the maximum velocity of the swirl sheath both increase. There is a positive correlation between the outlet velocity of the cathode channel and the stiffness of the gliding arc. The swirl sheath can protect the gliding arc, and the protective effect is enhanced when the speed increases.

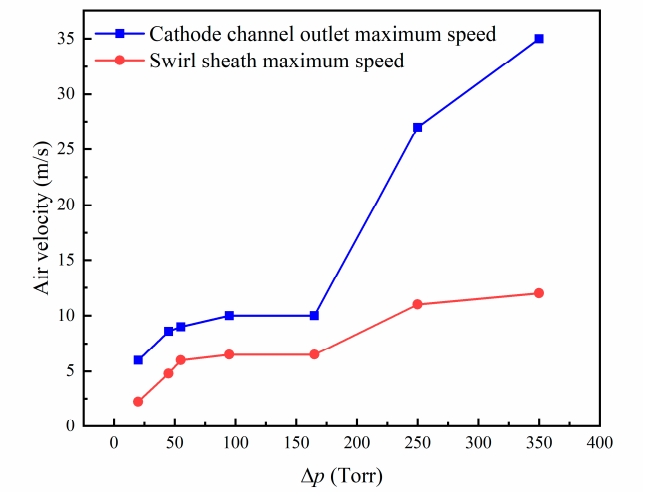

Figure 10. The maximum airflow velocity and the maximum swirl sheath velocity at the outlet of the cathode channel.

3.3. Jet Characteristics of the Gliding Arc Plasma Igniter

Figure 11 shows the variation in the maximum jet length with Δp. Figure 12 shows the maximum jet length of the gliding arc igniter captured by the high-speed camera at different values of Δp. When Δp is less than or equal to 50 Torr, the jet length of the gliding arc plasma igniter driven by differential pressure increases with the increase in Δp. The reason for this phenomenon is that as can be seen from the PIV test results, when Δp is small, the gas flow rate blown from the cathode channel is small and the airflow velocity is low, resulting in a small aerodynamic force acting on the gliding arc, which results in a short gliding arc jet. As Δp increases, the aerodynamic force acting on the gliding arc increases, and the length of the gliding arc jet increases accordingly.

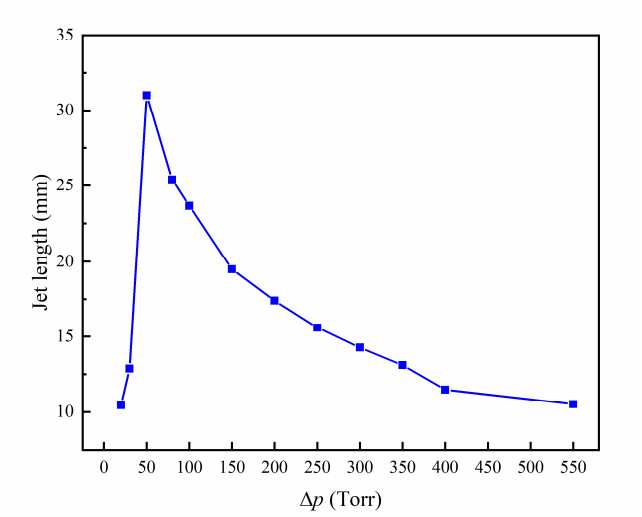

Figure 11. The relationship between jet length and Δp.

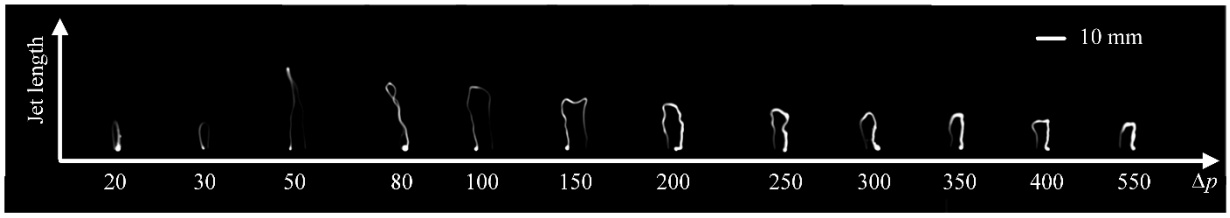

Figure 12. Maximum jet length of gliding arc captured by the high-speed camera at different Δp values.

When Δp is greater than 50 Torr, the jet length decreases with an increase in Δp. This is because when Δp is large, the gas flow rate and the gas flow velocity blown out from the cathode channel are large. Excessive gas flow will increase the thickness of the boundary layer in the cathode channel and reduce the cross-sectional area of the effective flow channel, which makes it difficult for the gliding arc to evolve and makes the gliding arc easy to break. When Δp is large, owing to the insufficient rigidity of the gliding arc, the gliding arc is continuously twisted and deformed under the action of the swirling gas and breaks. Therefore, the length of the jet cannot be continuously increased with the increase in the airflow.

When Δp is 50 Torr, the jet length reaches a maximum of 31 mm. However, at this time, the exit velocity of the igniter is small (about 9 m/s), the maximum velocity of the swirl sheath is about 6 m/s, and the rigidity of the gliding arc may be poor.

3.4. Ignition Characteristics of the Gliding Arc Plasma Igniter in the Hyperburner

Successful ignition and self-sustaining combustion are taken as the stable working standard for the hyperburner. Compared with the afterburner, the local flow rate of the hyperburner may be as high as 0.4 Ma, which introduces difficulties for stable ignition [32,33]; compared with the ramjet, the hyperburner has a lower temperature ($\leq$450 K) in the combustion chamber when flying at a small Ma, which leads to difficulty with respect to kerosene evaporation and ignition. In order to realize the stable operation of the hyperburner under low temperature and local high-speed conditions, the ignition characteristics of the hyperburner under the conditions of low temperature ($T^* \leq 450$ K) and 0.1 Ma are experimentally studied.

The timing of the ignition experiment is shown in Figure 13. Before the experiment, the total temperature of the incoming airflow, flow parameters, kerosene parameters, and parameters of the pressure difference between the inlet and outlet of the igniter were set. In the experiment, observations were made to determine whether a self-sustaining flame could be formed, and if a self-sustaining flame was formed, the ignition was considered successful. The experiment was repeated three times under the same working condition. If no stable flame was formed, it was considered that the working condition could not allow successful ignition. The ignition delay time is defined in the experiment as follows: The igniter starts timing when the igniter is energized. An initial fire nucleus will be formed in the initial stage of ignition, and the fire nucleus will continue to develop to form a flame front until the flame front propagates to the end of the observation window. At this time, the timer stops, and the recorded time is noted as the ignition delay time.

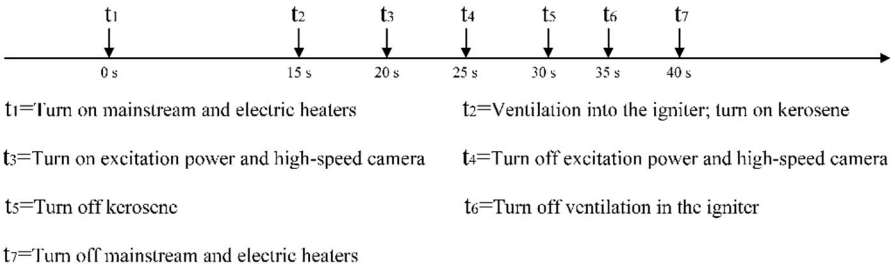

Figure 13. Hyperburner ignition test sequence.

3.4.1. Influence of Δp on Ignition Characteristics

There are many factors that affect the ignition performance of the gliding arc plasma igniter, among which the total temperature of the incoming flow, the oil–gas ratio, and the Δp are very important factors. Under the condition of an inlet flow rate of 0.1 Ma, the lean ignition limit of different inlet total temperatures and different Δp conditions is shown in Figure 14. The experiment showed that as the total inlet temperature decreases, the amount of kerosene required for successful ignition increases and the oil–gas ratio increases. When Δp is 550 Torr and the total inlet temperature is 450 K, the ignition can be successful with the oil–gas ratio of 0.0044; when Δp is 550 Torr and the total inlet temperature is 300 K, the ignition can be successful with the oil–gas ratio of 0.0072 (successful ignition oil–gas ratio increased by 38.9% compared to the total inlet temperature of 450 K). This is due to the decrease in the total inlet temperature resulting in a worsening effect of kerosene atomization and an increase in the proportion of kerosene particles with larger diameters. When kerosene particles with relatively larger diameters are ignited, they need to absorb more energy to atomize themselves to form kerosene particles with smaller diameters, which are then ignited by the gliding arc. The higher total incoming temperature not only contributes to the atomization of kerosene but also accelerates the chemical reaction rate of kerosene combustion.

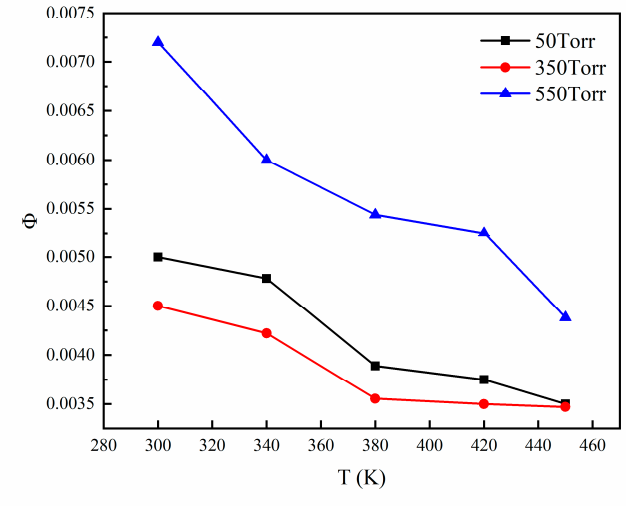

Figure 14. Lean ignition limit under different total inlet temperature and Δp conditions (Ma = 0.1).

In addition, Δp can affect the lean ignition limit. Under the three operating conditions of Δp of 50 Torr, 350 Torr, and 550 Torr, the widening effect of the lean ignition limit is the best when Δp is 350 Torr. When the total inlet temperature is 300 K, the oil–gas ratio is 0.0045, and Δp = 350 Torr, the hyperburner is successfully ignited (the lean ignition limit is widened by 37.5% compared to Δp = 550 Torr).

Figure 15 shows the ignition process at different values of Δp when the incoming flow velocity is 0.1 Ma, the total incoming flow temperature is 420 K, and the oil–gas ratio is 0.0043. The experiment shows that the ignition delay time is 17 ms when Δp = 350 Torr and the flame propagation process is the fastest; compared with the ignition delay time of 20.5 ms when Δp = 50 Torr, the ignition delay time is shortened by 17%. The hyperburner failed to ignite successfully when Δp = 550 Torr.

It can be seen from Figures 11 and 12 that the jet length at Δp = 50 Torr is about 2.4 times greater than that at Δp = 350 Torr, but the flame propagation process is slower than that at Δp = 350 Torr. The reason may be that the rigidity of the gliding arc is insufficient although the jet length of the gliding arc is the longest when Δp = 50 Torr. Under the action of the mainstream hot gas, the gliding arc is seriously offset, which reduces the contact area between the gliding arc and the kerosene droplet and weakens the ignition effect of the gliding arc.

There are two reasons for the failure to ignite successfully when Δp = 550 Torr. The first one is that increasing Δp will blow out a large amount of gas from the outlet of the cathode channel of the igniter, which will seriously damage the oil mist field near the outlet of the igniter and reduce the contact between the gliding arc and the kerosene droplets. Therefore, the ignition effect of the gliding arc is weakened. The second one is that the gas introduced into the igniter comes from the gas cylinder, and the gas temperature in the gas cylinder is lower than the incoming temperature. The larger Δp causes a large amount of low-temperature airflow to be ejected from the cathode channel, and the low-temperature airflow continues to act on the flow field near the igniter outlet, reducing the temperature near the igniter outlet and weakening the atomization effect of the high-temperature inflow on kerosene droplets.

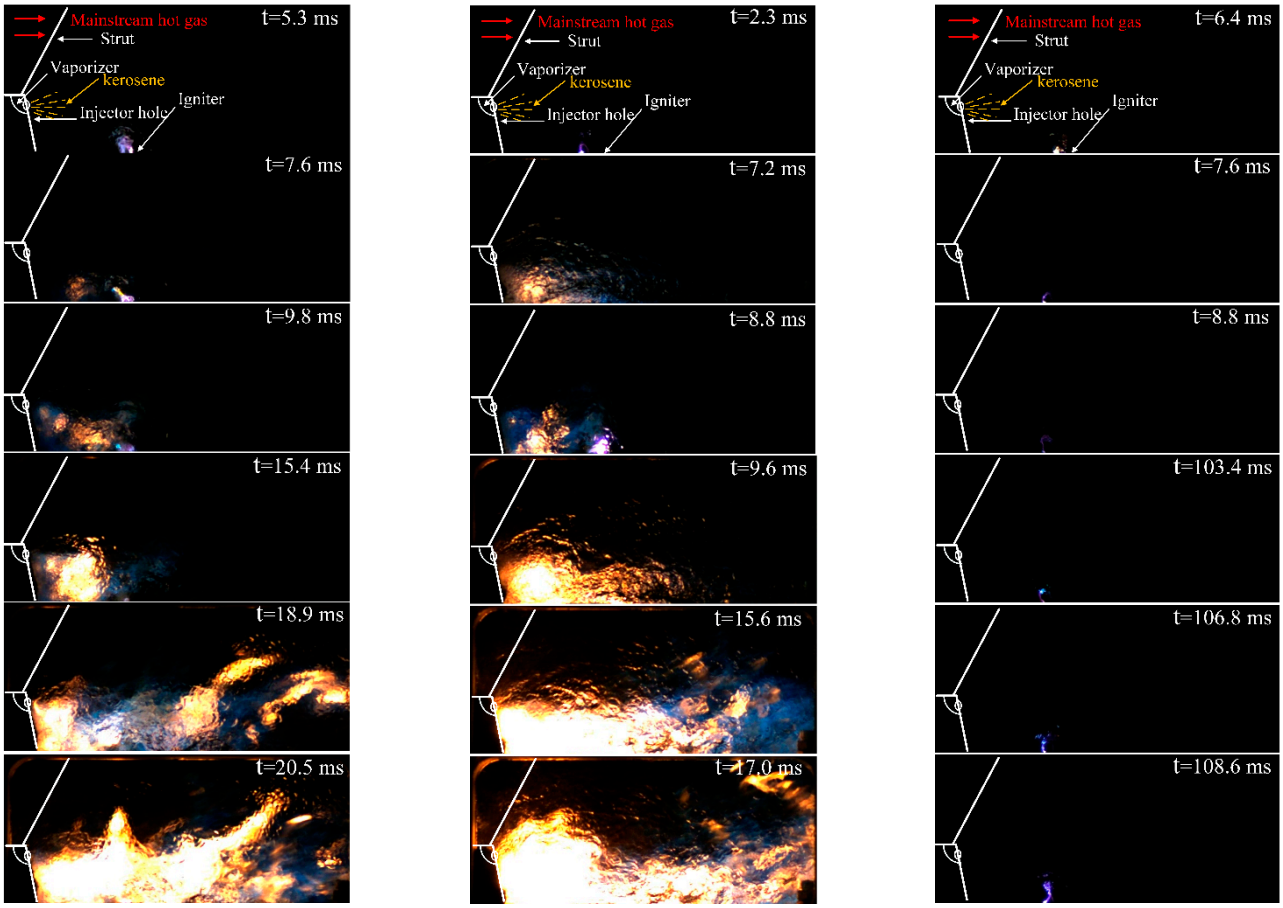

Figure 15. Ignition process at different Δp values: (**a**) Δp = 50 Torr; (**b**) Δp = 350 Torr; (**c**) Δp = 550 Torr.

3.4.2. Influence of Oil–Gas Ratio on Ignition Characteristics

Figure 16 shows the effect of using different oil–gas ratios on the flame propagation process when the inflow velocity is 0.1 Ma, the total inflow temperature is 420 K, and Δp is 350 Torr. When the oil–gas ratio is 0.0035, the flame is clearly blue-purple in the early stages of development, and the ignition delay time is about 104.5 ms; when the oil–gas ratio is 0.0043, the flame is clearly yellow-red in the early stages of development, and the ignition delay time is about 7.2 ms. The ignition delay time is decreased by 93.1% when compared to the case where the oil–gas ratio is 0.0035. The experiment results showed that when the oil and gas ratio is higher, the flame combustion is more sufficient than that in the case where the oil is leaner, the flame development speed is accelerated, and the ignition delay time is decreased.

The main reason for this phenomenon is that the kerosene droplets are blown out from the oil injection holes on the evaporation tank, and the kerosene droplets are rolled back to the vicinity of the igniter outlet under the action of the main recirculation area. The gliding arc quickly ignites the kerosene droplets near the outlet of the igniter. With the help of the gliding arc's own temperature and the heat generated by the combustion, the kerosene droplets are continuously evaporated and participate in the combustion. The initial fire core develops towards the injector hole under the action of the main recirculation area and the flame front propagates forward. Finally, the initial fire core forms a self-sustaining flame and fills the entire hyperburner. When the oil and gas ratio is relatively lower, the pressure atomization effect is poor, and the diameter of the kerosene droplets blown out of the injection hole is large and is not conducive to ignition. When the gliding arc interacts with the larger-diameter kerosene droplets, the gliding arc needs to first evaporate the

kerosene droplets into smaller-diameter droplets through its own heat to form a fire nucleus. When the oil and gas ratio is lower, there are large-diameter kerosene droplets around the initial fire nucleus, and the initial fire nucleus is easily submerged by the kerosene droplets, resulting in insufficient combustion around the initial fire nucleus, and the flame is observed to be blue-purple. As the combustion continues, the combustion releases a high level of heat, and the heat evaporates the larger-diameter kerosene droplets to form small-diameter kerosene droplets that are easy to burn, and the flame also changes from blue-purple to yellow-red. When the oil and gas ratio is larger, the pressure atomization effect is better, and a large number of kerosene droplets with small diameters are sprayed from the injection holes. When the kerosene droplet contacts the gliding arc, it can be instantly ignited and form a stable fire nucleus, and the flame is observed to be yellow-red. The initial fire nucleus develops rapidly, and the flame eventually fills the entire combustion chamber. Compared with the lean ignition state, when the oil–gas ratio increases, the ignition delay time and the flame development time are significantly reduced, which is more conducive to the formation of a self-sustaining flame.

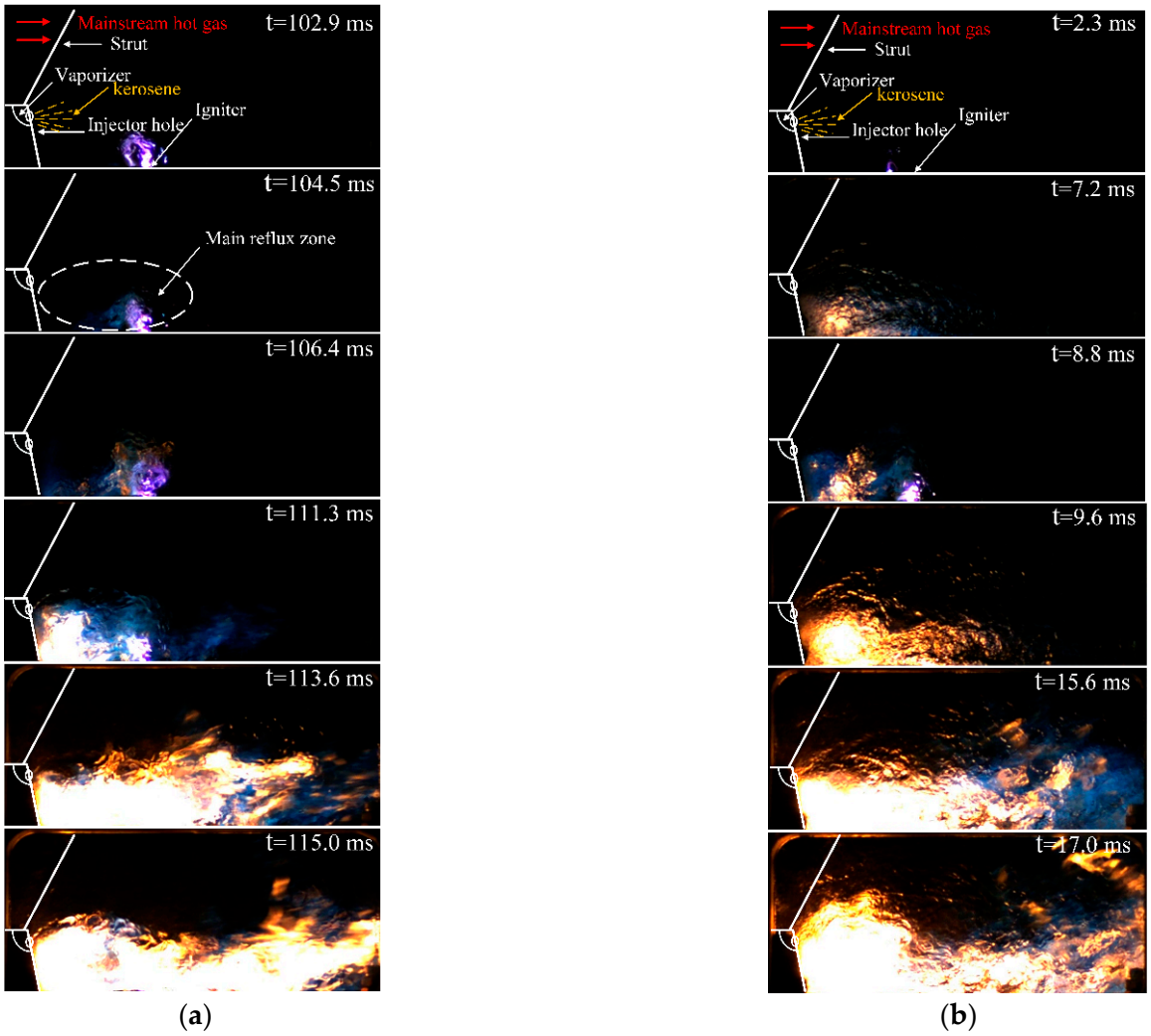

Figure 16. Flame propagation process under different oil–gas ratios (Ma = 0.1, total inlet temperature 420 K, Δp = 350 Torr): (**a**) oil–gas ratio: 0.0035; (**b**) oil–gas ratio: 0.0043.

4. Conclusions and Outlook

In this study, a gliding arc plasma igniter and a hyperburner-integrated flameholder are designed according to the working and structural characteristics of the hyperburner. This study innovatively proposes a new parameter (the pressure difference between the inlet and outlet of the igniter, Δp) that affects the operation of the gliding arc. The electrical characteristics, jet characteristics, and flow field characteristics of the gliding arc plasma igniter under different pressure differences were investigated experimentally. The ignition ability of the gliding arc plasma in the hyperburner was verified by experiments. The main conclusions are as follows:

(1) With the increase in Δp, the frequency of the trapezoidal envelope in the voltage and current waveforms increases, which means the frequency of the evolution and fracture of the gliding arc increases. When Δp is 550 Torr, it will affect the continuous discharge time of the gliding arc. There exists a period where the voltage is normal and the current is equal to 0 A. The appearance of this phenomenon may weaken the ignition effect of the gliding arc.

(2) The gas ejected from the cathode channel of the gliding arc plasma igniter driven by pressure difference will form a swirl sheath to protect the gliding arc at the igniter outlet. As Δp increases, the maximum velocity of the swirl sheath and the protective effect of the swirl sheath improve. The addition of Δp will raise the maximum airflow velocity of the gas ejected from the cathode channel, which helps to enhance the rigidity of the gliding arc.

(3) The length of the gliding arc jet tends to increase first and then decrease with the increase in Δp. When Δp is 50 Torr, the jet length reaches a maximum value of 31 mm while the exit velocity of the igniter (about 9 m/s) and the maximum velocity of the swirl sheath (about 6 m/s) are relatively small, indicating the gliding arc rigidity is relatively poor. The jet length of the gliding arc and the rigidity of the gliding arc should be considered in detail when the gliding arc is used in the ignition application of the hyperburner.

(4) The value of Δp can affect the lean ignition limit and ignition delay time of the hyperburner. When the incoming flow is 0.1 Ma and the inlet temperature is 300 K, the lean ignition limit can be widened by 37.5% when a Δp value of 350 Torr is compared with a Δp value of 550 Torr. When the inflow velocity is 0.1 Ma, the total inflow temperature is 420 K, and the oil–gas ratio is 0.0043, the ignition delay time is 17 ms when Δp is 350 Torr, and the flame propagation process is the quickest. Compared with the ignition when Δp is 50 Torr where the delay time is 20.5 ms, the ignition delay time is shortened by 17% when Δp is 350 Torr.

The results show that the application of gliding arc plasma in the hyperburner is extremely promising and the gliding arc can be considered as a new ignition method in the hyperburner. In addition, the ignition effect of gliding arc plasma igniters at a higher Mach number should be investigated. At the same time, in order to improve the ignition effect of the sliding arc plasma igniter, the output power of the excitation source can be increased or the power supply mode can be changed. In order to improve the rigidity of the gliding arc, the internal structure of the gliding arc igniter can be changed to optimize the plasma release process of the gliding arc. Moreover, the ignition effect of the gliding arc plasma igniter in different ignition positions needs to be tested and the optimal ignition position needs to be found.

Author Contributions: Conceptualization, X.C. and H.S.; methodology, X.C. and H.S.; software, X.C. and J.S.; investigation, W.C. and M.J.; data curation, X.C. and Z.Z.; writing—original draft preparation, X.C.; writing—review and editing, X.C.; supervision, H.S., D.J. and Y.Z. All authors have read and agreed to the published version of the manuscript.

Funding: This work was supported by the Natural Science and Technology Major Project (No. 2017-III-0008-0034) and Natural Science and Technology Major Project (No. 2019-III-0013-0015).

Institutional Review Board Statement: Not applicable.

Informed Consent Statement: Not applicable.

Data Availability Statement: Not applicable.

Conflicts of Interest: The authors declare no conflict of interest.

Nomenclature

Symbol	Description	Unit
Δp	Igniter inlet and outlet pressure difference	Torr
Ma	Mach number	-
T*	Hyperburner inlet total temperature	K

References

1. Chen, D.G. Brief Introduction of Hyperson Flight and TBCC Concept. *Aeroengine* **2006**, *32*, 4. (In Chinese)
2. Chen, M.; Tang, H.L.; Zhu, D.M.; Zhu, Z. Hypersonic combined cycle engine concept with tandem layout. *J. Beijing Univ. Aeronaut. Astronaut.* **2007**, *33*, 4. (In Chinese)
3. Marshall, A.; Gupta, A.; Lavelle, T.; Lewis, M. Critical Issues in TBCC Modeling. In Proceedings of the 40th AIAA/ASME/SAE/ASEE Joint Propulsion Conference and Exhibit, Fort Lauderdale, FL, USA, 11–14 July 2004.
4. Wang, Z.X.; Liu, Z.W.; Wang, M.; Li, B. Future Development and Application Prospect of Turbine Based Combined Cycle Engine. *Aeroengine* **2013**, *39*, 6. (In Chinese)
5. Mcnelis, N.; Bartolotta, P. Revolutionary Turbine Accelerator (RTA) Demonstrator. In Proceedings of the AIAA/CIRA 13th International Space Planes and Hypersonics Systems and Technologies Conference, Capua, Italy, 16–20 May 2005.
6. Jin, J.; Chen, M. Brief Introduction on Technology Development of Turbine Based Combined Cycle Engine. *Aeronaut. Manuf. Technol.* **2014**, *9*, 32–35. (In Chinese)
7. Stueber, T.J.; Vrnak, D.R.; Le, D.K.; Ouzts, P.J. *Control Activity in Support of NASA Turbine Based Combined Cycle (TBCC) Research*; NASA/TM 2010-216109; NASA: Washington, DC, USA, 2010.
8. Anderson, E.; Lopata, J. Using a modified SR-71 aircraft and air-launched expendable rockets to place small payloads into orbit. In Proceedings of the Joint Propulsion Conference & Exhibit, Lake Buena Vista, FL, USA, 1–3 July 1996.
9. Kloesel, K.J.; Ratnayake, N.A.; Clark, C.M. A Technology Pathway for Airbreathing, Combined-Cycle, Horizontal Space Launch Through SR-71 Based Trajectory Modeling. In Proceedings of the 17th AIAA International Space Planes and Hypersonic Systems and Technologies Conference, San Francisco, CA, USA, 11–14 April 2011.
10. Wang, D.; Chen, W.; Shao, J.W.; Hu, Y.C. Development of turbo-stamping combined propulsion technology and its application in near space. *Aerodyn. Missile J.* **2008**, *8*, 55–59. (In Chinese)
11. Lee, J.H.; Winslow, R.; Buehrle, R.J. *The GE-NASA RTA Hyperburner Design and Development*; NASA/TM 2005-213803; NASA: Washington, DC, USA, 2005.
12. Dimitrakellis, P.; Faubert, F.; Wartel, M.; Gogolides, E.; Pellerin, S. Plasma Surface Modification of Epoxy Polymer in Air DBD and Gliding Arc. *Processes* **2022**, *10*, 104. [CrossRef]
13. Pang, Y.; Hammer, T.; Müller, D.; Karl, J. Investigation of Nonthermal Plasma Assisted Charcoal Gasification for Production of Hydrogen-Rich Syngas. *Processes* **2019**, *7*, 114. [CrossRef]
14. Brande, W.T., IV. The Bakerian Lecture: On Some New Electro-Chemical Phenomena. *Philos. Trans. R. Soc. Lond.* **1814**, *104*, 51–61.
15. Jacobsen, L.S.; Carter, C.D.; Jackson, T.A.; Williams, S.; Barnett, J.; Bivolaru, D.; Kuo, S.; Tam, C.-J.; Baurle, R.A. Plasma-Assisted Ignition in Scramjets. *J. Propuls. Power* **2008**, *24*, 641–654. [CrossRef]
16. Huang, S.; Wu, Y.; Song, H.; Zhu, J.; Zhang, Z.; Song, X.; Li, Y. Experimental investigation of multichannel plasma igniter in a supersonic model combustor. *Exp. Therm. Fluid Sci.* **2018**, *99*, 315–323. [CrossRef]
17. Starikovskaia, S.M. Plasma assisted ignition and combustion. *J. Phys. D-Appl. Phys.* **2006**, *39*, R265–R299. [CrossRef]
18. Lin, B.; Wu, Y.; Zhang, Z.; Bian, D.; Jin, D. Ignition enhancement of lean propane/air mixture by multi-channel discharge plasma under low pressure. *Appl. Therm. Eng.* **2019**, *148*, 1171–1182. [CrossRef]
19. Ju, Y.G.; Sun, W.T. Plasma assisted combustion: Dynamics and chemistry. *Prog. Energy Combust. Sci.* **2015**, *48*, 21–83. [CrossRef]
20. Song, F.; Wu, Y.; Xu, S.; Jin, D.; Jia, M. N-decane decomposition by microsecond pulsed DBD plasma in a flow reactor. *Int. J. Hydrogen Energy* **2019**, *44*, 3569–3579. [CrossRef]
21. Starikovskii, A.Y. Plasma supported combustion. *Proc. Combust. Inst.* **2005**, *30*, 2405–2417. [CrossRef]
22. Czernichowski, A.; Nassar, H.; Ranaivosoloarimanana, A.; Fridman, A.A.; Simek, M.; Musiol, K.; Pawelec, E.; Dittrichova, L. Spectral and Electrical Diagnostics of Gliding Arc. *Acta Phys. Pol. A* **1996**, *89*, 595–603. [CrossRef]
23. Fridman, A.; Gutsol, A.; Gangoli, S.; Ju, Y.; Ombrello, T. Characteristics of Gliding Arc and Its Application in Combustion Enhancement. *J. Propuls. Power* **2008**, *24*, 1216–1228. [CrossRef]
24. Sun, W.; Uddi, M.; Ombrello, T.; Won, S.H.; Carter, C.; Ju, Y. Effects of Non-Equilibrium Plasma Discharge on Counterflow Diffusion Flame Extinction. *Proc. Combust. Inst.* **2011**, *33*, 3211–3218. [CrossRef]

25. Sun, W.; Uddi, M.; Won, S.H.; Ombrello, T.; Carter, C.; Ju, Y. Kinetic Effects of Non-Equilibrium Plasma-Assisted Methane Oxidation on Diffusion Flame Extinction Limits. *Combust. Flame* **2012**, *159*, 221–229. [CrossRef]
26. Ombrello, T.; Qin, X.; Ju, Y.; Gutsol, A.; Fridman, A.; Carter, C. Combustion Enhancement Via Stabilized Piecewise Nonequilibrium Gliding Arc Plasma Discharge. *AIAA J.* **2006**, *44*, 142–150. [CrossRef]
27. Ombrello, T.; Won, S.H.; Ju, Y.; Williams, S. Flame Propagation Enhancement by Plasma Excitation of Oxygen. Part I: Effects of O3. *Combust. Flame* **2010**, *157*, 1906–1915. [CrossRef]
28. Leonov, S.; Yarantsev, D.; Napartovich, A.; Kochetov, I. Plasma-Assisted Ignition and Flameholding in High-Speed Flow. In Proceedings of the 44th AIAA Aerospace Sciences Meeting and Exhibit, Reno, NV, USA, 9–12 January 2006; p. 563.
29. Leonov, S.; Houpt, A.; Elliott, S.; Hedlund, B. Ethylene Ignition and Flameholding by Electrical Discharge in Supersonic Combustor. *J. Propuls. Power* **2017**, *34*, 499–509. [CrossRef]
30. Leonov, S.B.; Yarantsev, D.A. Plasma-induced ignition and plasma-assisted combustion in high-speed flow. *Plasma Sources Sci. Technol.* **2006**, *16*, 132–138. [CrossRef]
31. Pinto, A.J.; Sagás, J.C.; Lacava, P.T. Repetition frequency of a DC gliding arc discharge in plasma-assisted fuel-rich combustion. *Europhys. Lett.* **2018**, *123*, 65001. [CrossRef]
32. Jia, M.; Lin, D.; Huang, S.; Zhang, Z.; Cui, W.; Wang, W. Experimental investigation on gliding arc plasma ignition in double-head swirling combustor. *Aerosp. Sci. Technol.* **2021**, *113*, 106726. [CrossRef]
33. Chen, W.; Jin, D.; Cui, W.; Huang, S. Characteristics of Gliding Arc Plasma and Its Application in Swirl Flame Static Instability Control. *Processes* **2020**, *8*, 684. [CrossRef]